Indonesian Journal of Electrical Engineering and Computer Science
Vol. 15, No. 1, July 2019, pp. 247~257
ISSN: 2502-4752, DOI: 10.11591/ijeecs.v15.i1.pp247-257

Active contour model for satellitale image segmentation using a local and global signed pressure force

Mouri Hayat, Fizazi Hadria
Faculté des mathématiques et informatique, Université des Sciences et de la Technologie Mohamed Boudiaf, Algeria

Article Info

Article history:

Received Sep 07, 2018
Revised Nov 17, 2018
Accepted Mar 2, 2019

Keywords:

Global signed pressure force
Image segmentation
Intensity inhomogeneity
Lif model
Local

ABSTRACT

Global and local image information is crucial for accurate segmentation of images with intensity inhomogeneity valuable minute details and multiple objects with various intensities. We propose a region-based active contour model which is able to utilize together local and global image information. The major contribution of this paper is to expand the LIF model which is includes only local image information to a local and global model. The introduction of a new local and global signed pressure force function enables the extraction of accurate local and global image information and extracts multiple objects with several intensities. Several tests performed on some synthetic and real images indicate that our model is effective as well as less sensitivity to the initial contour location and less time compared with the related works.

Corresponding Author:

Mouri Hayat,
Faculté des mathématiques et informatique,
Université des Sciences et de la Technologie Mohamed Boudiaf,
Oran, Algeria.
Email: hayat.mouri @univ-usto.dz

1. INTRODUCTION

It is quite normal that the crucial step needed for many vision applications by computer and image processing is Segmentation of images. Within this framework, this paper aims at developing models dealing with problems of detecting objects (segmenting images) characterized by intensity inhomogeneity which represents an intensity variation in the regions of images and makes segmentation difficult. Divergent techniques have been proposed [1-2] and currently, active contour model (ACM) [1, 3-6] is the most method used in image processing in view of the quality and of the results it offers. In fact, the basis of the ACM is evolving a curve under some constraints from a given image to match the shape of the desired objects, by minimizing energy functional. Theoretically, ACMs are classified into two main categories: edge-based [1, 3, 4, 6, 7-10] and region-based [5, 11-17].

The primary work of Edge-based models is the detection of contours which approximate discontinuities of the gray level, color, texture. So they use the gradient image by evolving the curve to reach the edges of interest object. Within this type, geodesic active contour (GAC) [4] is one of the most accurate techniques. GAC meets difficulty when dealing with the objects having blurred or discrete boundaries and it hardly segments the object corrupted by noise [18], although it has been effectively applied for images with high variation in gradient at the contours of the objects.

Unlike edge-based models that look for dissimilarities, the region-based models rather look for similarity. These approaches provide a map of closed areas. They utilize image statistics inside and outside the curve to control the evolution. One of the famous region-based models is the [5] which is a simplified Mumford-Shah model [12]. The C-V model utilizes the global property of homogeneous regions. Thus, it has

good segmentation result for the objects with weak or discrete contours but often fails when the intensity inhomogeneity is present in image [19].

Some works using local image property are cited such as presented by Li et al in [19-20] and Wang et al in [22]. Li et al introduces a local binary fitting (LBF) energy by using local mean intensity property instead of global ones. Furthermore, Wang et al illustrates Local image intensities by local Gaussian distributions (LGD). Therefore, this two models gives more robustness when the inhomogeneity dominates the images. However, they can be falling in local minimums and in addition the result is more dependent on the contour initialization.

In [23] a local image fitting model is presented for segmenting images with no uniform intensity where the authors define the local image property on the differences between the fitting image [20-21] and the original one. Additionally, Gaussian filtering is introduced for regularizing the level-set function. It ensures a uniform evolution equation, and eliminates the requirement of resetting the curve evaluation, which is very computationally expensive.

Other hand, a region-based active contour methods are formulated in [24-25, 28] by utilizing a signed pressure force (SPF) function based on the two global and local intensity means respectively. The first model is used in order to handle non homogeneity. However, the second model is effective for noisy images. The Gaussian kernel is introduced in their equation of level set to stabilize it. Thus, it doesn't require re-initialization at each step.

Our contribution is to present a new a local (ACM) inspired from [23]. Our method is not based only on the local property of the fitted image but we will also consider the global one. Furthermore, we multiply the difference local and global fitted images expressions to formulate the energy functional. After minimizing this functional, we replace the difference local and global fitted images with the local and global signed pressure force (SPF) functions in the variational level set equation. Both local and global (SPF) functions are used for detecting regions with intensity inhomogeneous and ones homogenous respectively. For reducing the computational time and accelerate the convergence of the evolution equation, we apply the Gaussian kernel to regularize the contour at each iteration.

2. RELATED WORK

2.1. Chan-Vese (CV) Model

The energy of CV model is given as follow:

$$F^{CV}(C,c_1,c_2) = \lambda_1 \int_{outside(C)} |I(x)-c_1|^2\,dx + \lambda_2 \int_{inside(C)} |I(x)-c_2|^2\,dx + v|C| \quad (1)$$

Where outside (C) and inside (C) represents the regions outside and inside the curve C, respectively. c1 and c2 designate two constants that approximate the image intensities in outside(C) and inside (C), respectively. λ_1, λ_2 are fixed constants. The third term is the length of the curve. After minimizing (1) by using the descent gradient [27], the (1) is expressed as the zero level set evolution curve and the corresponding level set equation is :

$$\frac{\partial \phi}{\partial t} = \delta(\phi)\left[\mu div\left(\frac{\nabla \phi}{|\nabla \phi|}\right) - v - \lambda_1 (I-c_1)^2 + \lambda_2 (I-c_2)^2\right] \quad (2)$$

where c1 and c2 can be updated at every iteration by:

$$c_1(\phi) = \frac{\int_\Omega IH(\phi)d\Omega}{\int_\Omega H(\phi)d\Omega} \quad (3)$$

$$c_2(\phi) = \frac{\int_\Omega I(1-H(\phi))d\Omega}{\int_\Omega (1-H(\phi))d\Omega}$$

In practice, the Heaviside function and Dirac function are smoothed by:

$$H(x)=\begin{cases}1, x\geq 0\\ 0, x<0\end{cases} \tag{4}$$

$$\delta(x)=\frac{d}{dx}H(x) \tag{5}$$

Because the CV model uses the global property so they give to CV model a good performance when segmenting images with weak edges and noise. However it fails when the inhomogeneity strongly exists in the image since it doesnt incorporate local property.

2.2. Local Binary Fitted (LBF) Model

The LBF model which is proposed by Li et al. in [20-21] utilizes two spatially varying fitting functions f1(x) and f2(x) to approximate the local intensities on the two sides of the contour. And the image fitting energy function was defined as follows:

$$E_{LBF}=\lambda_1\int_{\Omega}\left[\int_{\Omega}K_{\sigma}(x-y)|I(y)-f_1(x)|^2H(\phi(y))dy\right]dx + \lambda_2\int_{\Omega}\left[\int_{\Omega}K_{\sigma}(x-y)|I(y)-f_2(x)|^2(1-H(\phi(y)))dy\right]dx \tag{6}$$

where (λ1, λ2) are positive fixed parameters. Kσ is a Gaussian kernel with standard deviation σ, and f1 and f2 are two smooth functions that approximate the local image intensities inside and outside curve C, respectively.

Minimizing the energy functional ELBF with respect to ϕ, the gradient descent flow is defined as follows:

$$\frac{\partial\phi}{\partial t}=-\delta(\phi)(\lambda_1e_1-\lambda_2e_2)+v\delta_{\varepsilon}(\phi) \tag{7}$$

Where e1 and e2 are defined as:

$$e_1(x)=\int_{\Omega}K_{\sigma}(x-y)|I(y)-f_1(x)|^2dy$$
$$e_2(x)=\int_{\Omega}K_{\sigma}(x-y)|I(y)-f_2(x)|^2dy \tag{8}$$

Functions f1 and f2 are the local intensity means inside and outside curve C, which are computed in a local region:

$$f_1(x)=\frac{K_{\sigma}(x)*[H_{\varepsilon}(\phi(x))I(x)]}{K_{\sigma}(x)*H_{\varepsilon}(\phi(x))}$$
$$f_2(x)=\frac{K_{\sigma}(x)*[1-H_{\varepsilon}(\phi(x))I(x)]}{K_{\sigma}(x)*[1-H_{\varepsilon}(\phi(x))]} \tag{9}$$

The LBF method could properly segment a homogeneous object from the inhomogeneous background. Since it uses local property, it is easy to be attrapped in minima local. So, it strongly dependent on initial contour position [27].

2.3. Local Image Fitted (LIF) Model

The LIF model proposed by Zhang et al. [23] utilizes the local image property to form an energy function, which is written as:

$$E^{\mathrm{LIF}} = \frac{1}{2}\int_{\Omega} \left|\mathrm{I}(\mathrm{x}) - \mathrm{I}^{\mathrm{LFI}}(\mathrm{x})\right|^2 \mathrm{dx}, \mathrm{x} \in \Omega \tag{10}$$

The energy function is based on the difference between the local fitting image and the original image [23]. The local fitting image is defined as follows:

$$I^{LFI} = m_1 H(\phi) + m_2(1 - H(\phi)) \tag{11}$$

Where m1 and m2 are expressed as:

$$\begin{cases} m_1 = mean(I \in ((x \in \Omega | \phi(x) > 0) \cap w_k(x))) \\ m_2 = mean(I \in ((x \in \Omega | \phi(x) < 0) \cap w_k(x))) \end{cases} \tag{12}$$

Wk is a window function. By minimize the energy functional with respect to level set function ϕ, we can obtain:

$$\frac{\partial \phi}{\partial t} = \delta_{\varepsilon}(\phi).(I - I^{LFI})(m_1 - m_2) \tag{13}$$

where $\delta_{\varepsilon}(\phi)$ is the regularized Dirac (5).

3. PROPOSED METHOD

In order to segment intensity inhomogeneous images, the following energy functional is defined:

$$E_{gLGFI} = E_{LGFI}(\phi) + \mu L_g(\phi) + \nu A_g(\phi) \tag{14}$$

$\mu \geq 0$ and $v \geq 0$ are fixed parameters. Lg(ϕ) and Ag(ϕ) are length and area terms, respectively [7] :

$$L_g(\phi) = \int_{\Omega} g(I)\delta_{\varepsilon}(\phi)|\nabla \phi| dx, \tag{15}$$

$$A_g(\phi) = \int_{\Omega} g(I) H_{\varepsilon}(-\phi) dx, \tag{16}$$

The energy function Ag(ϕ) is introduced to speed up the curve evolution. It is the area of the region $\Omega^{-}{}_{\phi} = \{(x,y) | \phi(x,y)| < 0 \}$. Ag(ϕ) can be viewed as the weighted area of $\Omega^{-}{}_{\phi}$.

In (16), g(I) is a positive monotonously decreasing edge indicator function ranging in [0, 1]:

$$g(I) = \frac{1}{1 + |\nabla K_{\sigma} * I|^2} \tag{17}$$

ELGFI is defined according to the following reformulation of (10):

$$E_{LGFI} = \int_{\Omega} \left(I(x) - I_{LFI}(x)\right)\left(I(x) - I_{GFI}(x)\right) dx \tag{18}$$

In (18), let ILFI(x) be a local fitted image and IGFI(x) a global fitted image, using a level set ϕ, which are defined as:

$$I_{LFI}(x) = f_1 M_1 + f_2 M_2, \tag{19}$$

$$I_{GFI}(x) = c_1 M_1 + c_2 M_2, \tag{20}$$

Where f1 and f2 are local intensity means and c1and c2are global intensity means of the given image as defined in (9) and (3), respectively.

$M_1 = H(\phi)$ and $M_2 = (1 - H(\phi))$, where H(ϕ) is the regularized Heaviside (4).

As follow, we present a hybrid model to deal the intensity inhomogeneity problem firstly and then ensure its convergence in computing time very reduced. ELGF in (18) is minimized with respect to ϕ, By using the calculus of variations and steepest gradient descent [26]:

$$\frac{\partial \phi}{\partial t} = \begin{pmatrix} (I(x) - I_{LFI}(x))(c1 - c2) + \\ + (I(x) - I_{GFI}(x))(f1 - f2) \end{pmatrix} \delta_\varepsilon(\phi), \tag{21}$$

{c1, c2} and {f1, f2} are global and local intensity means defined in (3) and (9), respectively. The terms $(I(x) - I_{LFI}(x))(c1 - c2)$ and $(I(x) - I_{GFI}(x))(f1 - f2)$ in (21) are replaced by local and global signed pressure force (SPF) functions because the above equation is not stable around object boundaries and doesn't give a good segmentation when the contours of inhomogeneous objects and the background are inseparable. Thus it results an unstable contour. The evolution equation is proposed as follow:

$$\frac{\partial \phi}{\partial t} = \left(\lambda_1 L_{SPF}(c_1 - c_2) + \lambda_2 G_{SPF}(f_1 - f_2)\right) \tag{22}$$

where the proposed local and global SPF functions which normalize the values to [-1,1] are defined as:

$$L_{SPF} = \begin{cases} \dfrac{I(x) - I_{LFI}(x)}{max(|I(x) - I_{LFI}(x)|)}, & I(x) \neq 0 \\ 0, & I(x) = 0, \end{cases} \tag{23}$$

$$G_{SPF} = \begin{cases} \dfrac{I(x) - I_{GFI}(x)}{max(|I(x) - I_{GFI}(x)|)}, & I(x) \neq 0 \\ 0, & I(x) = 0, \end{cases} \tag{24}$$

By using the calculus of variations and steepest gradient descent, the solution of Eg,LGFI from (14) using (15) and (16) is:

$$\frac{\partial \phi}{\partial t} = \begin{pmatrix} \lambda_1 L_{SPF}(c_1 - c_2) + \lambda_1 L_{GPF}(f_1 - f_2) + \\ + \mu\, div\left(g \dfrac{\nabla \phi}{|\nabla \phi|}\right) + \upsilon_g \end{pmatrix} \delta_\varepsilon(\phi) \tag{25}$$

The two scaling parameters λ1and λ2in (22) and (25) are used to tune the model for different types of images. The SPF functions defined in (24) and (25) are used to normalize the local and global image differences in the range [-1, 1] inside and outside the region of interest. The new SPF functions proposed in this work are based on both global and local intensity-based fitted images.

Finally, the different steps of the proposed algorithm are as follows:

1. Initialization of the level sets function ϕ to be a binary function as follows:

$$\phi(x, t = 0) = \begin{cases} -\rho, & x \in \Omega_0 - \partial\Omega_0 \\ 0, & x \in \partial\Omega_0 \\ \rho, & x \in \Omega - \Omega_0 \end{cases} \tag{26}$$

where ρ is a positive constant, Ω_0 is the inner region of the initial contour, Ω is the image domain and $\partial\Omega_0$ refers to the initial contour.

2. Compute the edge indicator function g(I) using (17)
3. Compute the local intensity means, f1, f2, and the global means, c1, c2, using (9) and (3), respectively.
4. Calculate LSPF(I) and GSPF(I) using (23) and (24), respectively.
5. Solve the partial differential equation (PDE) of ϕ using (25).
6. Regularize the level-set function ϕ at time t by applying a Gaussian kernel Gχ, i.e. ϕ = Gχ*ϕ, where χ is the standard deviation of the regularizing Gaussian kernel.
7. Check whether the regularized level-set function is stationary. If not, iterate from step (3).

4. RESULTS AND ANALYSIS

In this section, we apply and compare the proposed model with the different models using both synthetic and real images. All models are implemented using Matlab 7.0 on Windows 7; on 2.3 GHz Intel core i5 PC with 6GB of RAM. Unless otherwise specified, the parameters are described in Table 1.

Figure 1 shows the segmentation results of the related methods and the proposed method on a synthetic image with two objects with blurred boundaries. From the first row, we can observe that all models can satisfactorily segment the two objects. Furthermore, the iterations and CPU time are listed in Table 2.

The second row of Figure 1 demonstrates the segmentation results. As shown, they cannot detect the boundaries of the two objects after the same number of iterations mentioned in Table 2. Figure 2 shows a segmentation result comparison with the related methods of image with intensity inhomogeneity.

Table 1. Description of the Parameters used in the Study

Parameters	Description
ρ	To initialize the level set function, $\rho > 0$ is a constant (LBF: ρ =1,:LIF: ρ =2 and our model : ρ =1).
σ or χ	Scale parameter in Gaussian kernel (LBF: σ =4, LIF: σ =3, χ =1and our model: σ=3, χ =0.5).
λ_1/λ_2	Weighting parameters (C-V, LBF: $\lambda 1 = \lambda 2$ =1 and Our model λ_1 =1, λ_2 =5).
Δt	Time step (LBF, Δt = 0.1; C-V, LIF and our model: Δt = 1).
ε	The parameter of smoothed Heaviside function (LBF, LIF and our model: ε = 1.5).
v ,μ	Area and length terms are regularization parameters of curve C (C-V: μ=0.2, v=0, LBF:μ=0.01and our model μ=1, v=0.25).

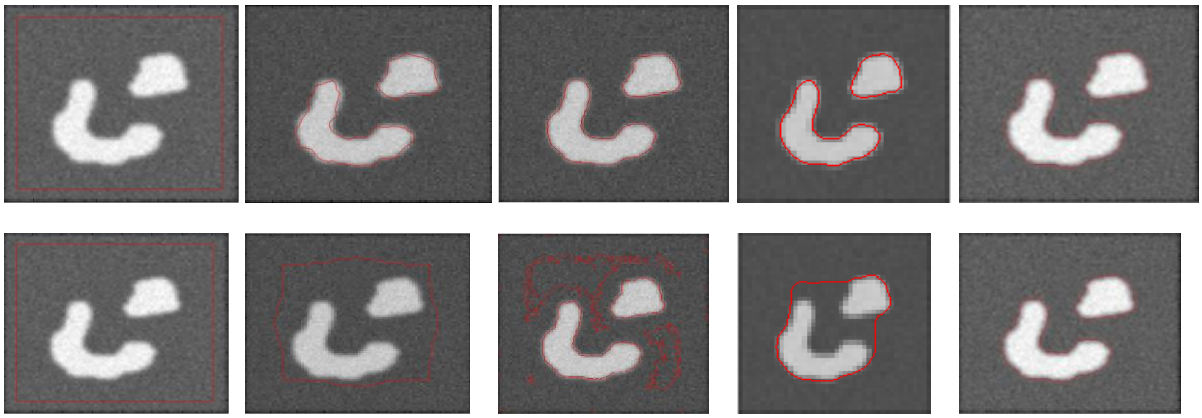

(a) (b) (c) (d) (e)

Figure 1. Segmentation results on a synthetic image: (a) initial contour, Segmentation result by: (b) the LIF model, (c) the LBF model, (d) the CV model and (e) the proposed model

Table 2. Iterations and CPU Time Needed by the Methods Compared when Segmenting the Image in Figure 1

Methods	iterations	CPU time (s)
The LIF model	40	2.48
The LBF model	50	3.29
The CV model	100	4.15
The proposed model	8	1.81

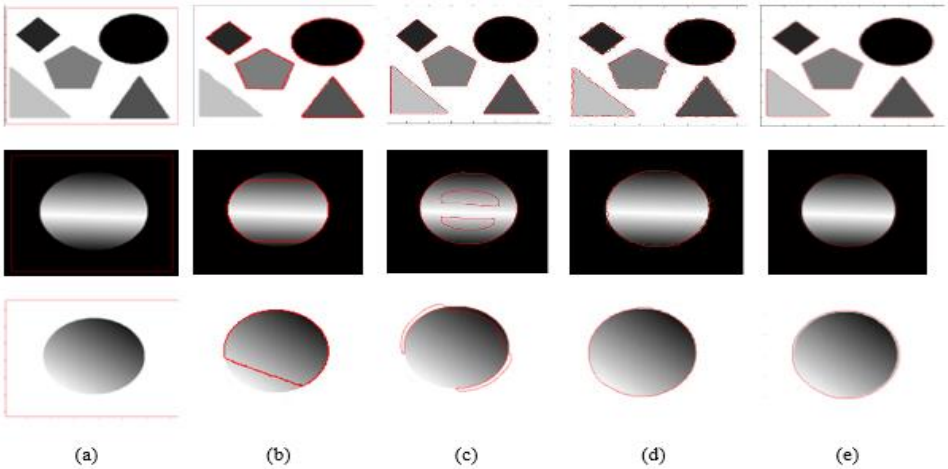

Figure 2. Comparison of segmentation results using synthetic image with intensity inhomogeneity (a) initial contour. Segmentation result by: (b) the CV model. (c) the LBF model. (d) the LIF model. (e) the proposed model

It can be seen that the methods using global region information (CV) cannot segment well when an image has an intensity inhomogeneous region in it. The segmentation results with LBF are shown inthe third column. This method is only able to properly segment the first image, while the segmentation results are not acceptable for the other images. The fourth column shows the segmentation results using LIF. This method is able to properly segment the first image. As for the second and the third image, the contour is not quite smooth along the boundary of the object. Although it is able to segment the object in the fourth image, some undesirable contour is stuck in the background. The last column shows the segmentation results using the proposed method, which is able to properly segment all images.

Figure 3 shows the experiments conducted with synthetic images with different types of region properties, we used an image with a single homogeneous object and then progressively changed its intensity distribution to a point at which it is even difficult to manually segment it, thus making the object inhomogeneous. The first row shows the five input images with the initial contour, whereas the segmentation results are shown using C-V [5] in the second row, LBF [13, 21] in the third row, LIF [23] in the fourth row and our model in the last row, respectively. Visual inspection clearly shows that the C-V method cannot segment well when an image has an intensity inhomogeneous region in it and both the proposed method and LBF provide the best segmentation results. LIF also yields acceptable segmentation results, although the final contour in this method is not quite smooth along the object boundaries. For all the examples in Figure 3, the parameters of all methods were kept constant.

In Figure 4, we apply all the tested methods to synthetic images with different initial contour. The first row shows various initial contours, the second, the third rows and the last row show the segmentation results by the LBF model, the LIF model and the proposed model, respectively. From some initial contours, as in column 1, the LBF model and the LIF model can segment well image, while giving bad segmentation results for other initial contours. Otherwise, the proposed model is much more robust to initial contour location and can achieve good segmentation results for all initial contours.

To quantitatively validate the segmentation performance of the proposed model from Figure 3, the Jaccard Similarity (JS) index is used. The JS index between the segmented object region Rs and the real object region Ro is calculated as $JS(R_S,R_O)=|R_S \cap Ro|/|Rs \cup Ro|$. Clearly, when Rs is more similar to Ro, the JS value is close to 1. Figure 5 shows that the JS values obtained by our method change in a small range for intensity inhomogeneity with different strength, while the LBF model and the LIF model, when the strength of intensity inhomogeneity is strong in last two rows of Figure 3 the segmentation accuracy of this method decreases strictly. These results illustrate the robustness of the proposed model to image intensity inhomogeneity.

In Figure 6, we apply the proposed model to segment typical remote sensing images with different modalities and compare it to CV, LBF and LIF models. The first row shows the four input images with red initial contour, whereas the segmentation results are shown using CV in the second row, LBF in the third row, LIF in the forth row and the proposed method in the last row, respectively. In the second row, it can be seen that the CV model fails in all given images because it's based on global properties of image. Although the other methods are based on the local properties of the image, they don't lead to a good segmentation.

Moreover, the LBF and the LIF models fail to distinguish between the intensity between the object and its background and lead to inaccurate segmentation results. But our method results are more satisfactory as it shown by green circle in the first row. So, it can segment more detailed regions than the other methods as shown by the green arrows. These results represent the abilities of the proposed model to deal with intensity inhomogeneity and complex background.

Figure 7 shows some segmentation results by applying the proposed method to differentintensity inhomogeneous noisy images. Although noise affected the crispness of edges in theinput data, the proposed method is able to yield acceptable segmentation results.

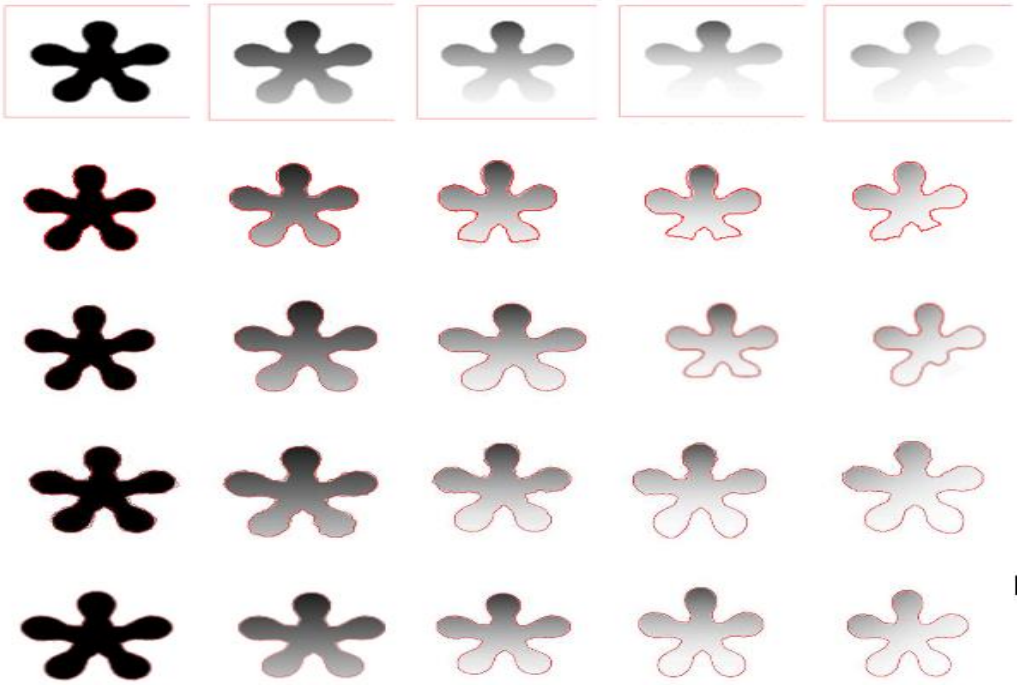

Figure 3. Segmentation results on a synthetic image where the strength of intensity inhomogeneity is gradually increased from left to right. Row1: input images with the initial contour. Row2: results of the CV model. Row3: results of the LBF model. Row4: results of the LIF model. Row5: results of the proposed model

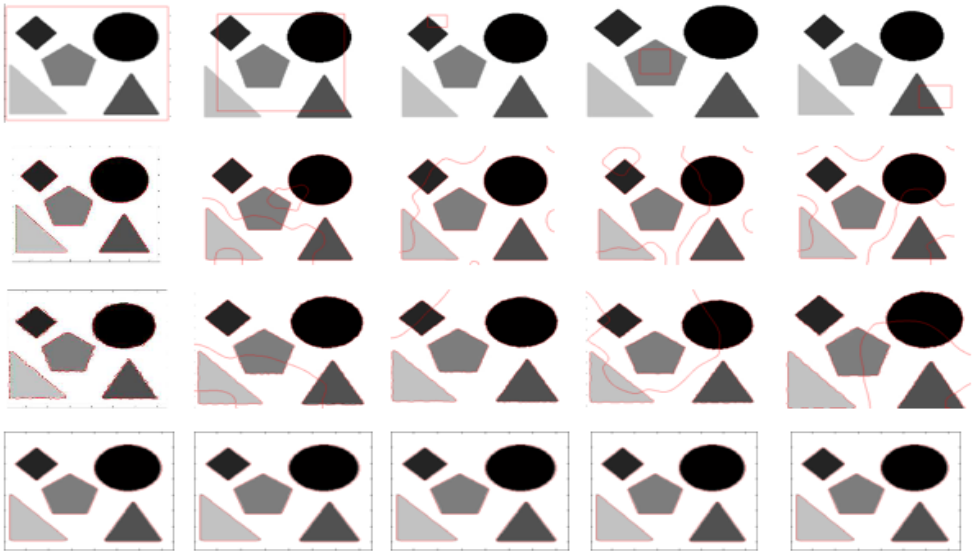

Figure 4. Effect of position of initial contour on the final segmentation results

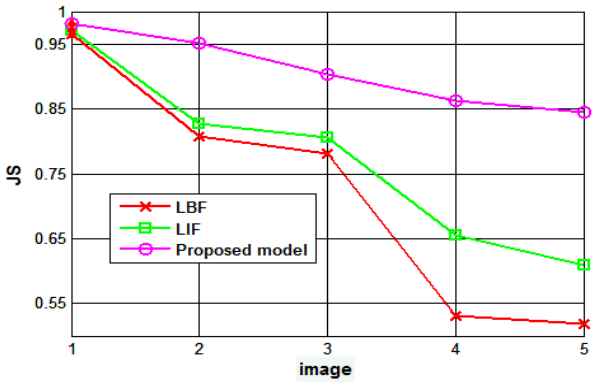

Figure 5. The corresponding JS values yielded by the LBF model, the LIF model and the proposed model on the five images with different intensity inhomogeneity

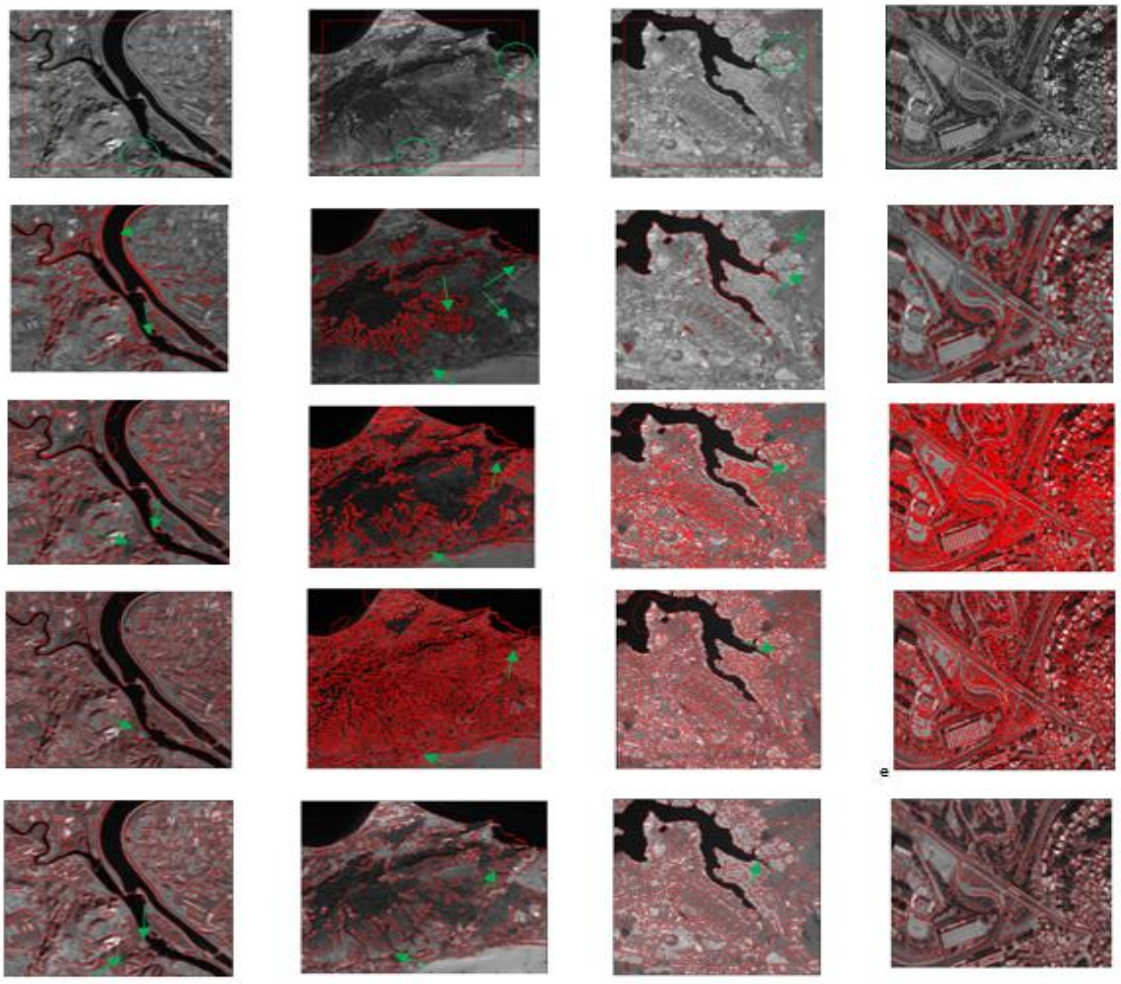

Figure 6. Segmentation results on remote sensing images. Row1: input images with red initial contour. Row2: results of the CV model. Row3: results of the LBF model Row4: results of the LIF model. Row5: results of the proposed model

First row original image added the salt and pepper noise with initial contour, second row final contour. Furthermore, the iterations and CPU time of segmenting the images in Figure 6 are listed in Table 3 for all models studied in this paper. The proposed method yields the lowest time complexity for the examples shown in rows 4 and 5. It takes 23.72 and 29.54 seconds for the examples shown in the last two rows,

respectively. On the other hand, CV and LBF have the lowest time complexity for the example shown in row 2 and 3. In row 2, they take 30.54 and 105.95 seconds respectively while the proposed method take 441.68 seconds to obtain the final contour. Similarly for row3, they take 27.65 and 52.27 seconds respectively while the proposed method take 96.06 seconds to obtain the final contour. Although CV and LBF have the lowest time complexity for this example, it is unable to properly segment the object as shown in Figure 6. Accordingly, the proposed model is much faster than the othermodels.

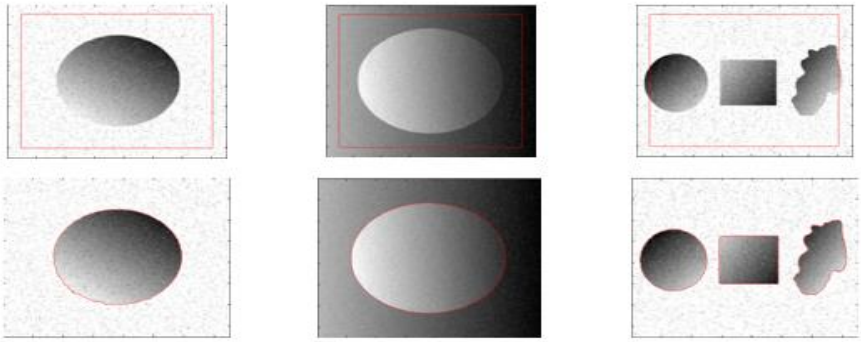

Figure 7. Segmentation results on a different intensity inhomogeneous noisy images

Table 3. Iterations and CPU Time for the Examples Shown in Figure 6

	Row2		Row3		Row4		Row5	
Models	Iterations	CPU time(s)	Iterations	CPU time(s)	Iterations	CPU time(s)	iterations	CPU time(s)
CV	800	**30.54**	900	**27.65**	900	29.67	1500	65.53
LBF	600	**105.95**	400	**52.27**	100	49.98	400	502.46
LIF	400	520.27	200	315.46	150	45.13	500	560.51
Our model	400	**441.68**	100	**96.06**	50	23.72	50	29.54

Active contour methods behave differently for different types of images. Because the synthetic images shown in Figure 3 have different characteristics compared to Satellitales images shown in Figure 6. The parameters used for all experiments in Figure 6 are shown in Table 4. For example, as shown in Table 4, the parameters are fixed at λ_1=5 and λ_2=1. So, λ_1 is higher than λ_2 because when the intensity inhomogeneity is severe like the images presented in Figure 6, the accuracy of segmentation relies on the local SPF, in such case, we choose a small λ_2; the local SPF becomes degenerating the global SPF so that the contour is attracted to the object boundary quickly. Similarly for the parameter σ, it is advisable to choose a small σ to segment the small object in further detail (in this case σ=3). The parameters had to be tuned in order to obtain the best possible segmentationresults.

Table 4. Parameters for the Experiments Needed when Segmenting Images in Figure 6

	λ_1	λ_2	μ	υ	σ	χ	ρ	ε	∇t
CV	1	1	0.2	0	-	-	1	1	0.1
LBF	1	1	0.001	-	4	-	1	1.5	0.1
LIF	-	-	-	-	3	1	2	1.5	1
Our model	5	1	1	0.25	3	0.5	1	1.5	0.1

5. CONCLUSION

We have presented a new ACM which is able to use globaland local image property for segmenting a range of images with intensity inhomogeneity. The main contribution of this paper is to expand the LIF model which is includes only local image information to a local and global in the variational level set formulation. We have also introduced the SPF function in the gradient descent solution to give more robustness to the final solution and extract multiple objects with several intensities. The tests results have shown that our method performs robustly in severe inhomogeneity and is effective as well as less sensitivity to the initial contour location and less time compared with the related works. In future we aim to extend it to multi-phase segmentation and we hope to reduce the computing time consuming.

REFERENCES

[1] M. Kass, A. Witkin, D. Terzopoulos, "Snakes: active contour models," *International Journal of Computer Vision*, 1988, 1, 321-331.

[2] N. Xu, N. Ahuia, R. Bansal, "Object segmentation using graph cuts based active contours," *Computer Vision and Image Understanding*, 2007, 107, 210-224.

[3] V. Caselles, R. Kimmel, G. Sapiro, "Geodesic active contours," in: *Processing of IEEE International Conference on Computer Vision*'95, Boston, 1995, MA,, pp. 694-699.

[4] V. Caselles, R. Kimmel, G. Sapiro, "Geodesic active contours", *International Journal of Computer Vision*, 1997, 22 (1) 61-79.

[5] T. Chan, L. Vese,, "Active contours without edges", *IEEE Transaction on Image Processing*, 2001, 10 (2), 266-277.

[6] G.P. Zhu, Sh.Q. Zhang, Q.SH Zeng, Ch.H. Wang, "Boundary-based image segmentation using binary level set method", *Optical Engineering, 2007, 46*, 050501.

[7] C.M. Li, C.Y. Xu, C.F. Gui, M.D. Fox, "Level set evolution without re-initialization: a new variational formulation," in: *IEEE Conference on Computer Vision and Pattern Recognition*, 2005, San Diego, pp. 430–436.

[8] N. Paragios, R. Deriche, "Geodesic active contours and level sets for detection and tracking of moving objects," *IEEE Transaction on Pattern Analysis and Machine Intelligence* 22, 2000, 1-15.

[9] C. Xu, J.L. "Prince, Snakes, shapes, and gradient vector flow," *IEEE Transaction on Image Processing*, 1998, 7, 359-369.

[10] Vasilevskiy, K. Siddiqi, "Flux-maximizing geometric flows," *IEEE Transaction on Pattern Analysis and Machine Intelligence, 2002, (24) 1565-1578.*

[11] J. Lie, M. Lysaker, X.C. Tai, "A binary level set model and some application to Munford–Shah image segmentation", *IEEE Transaction on Image Processing*, 2006, 15, 1171-1181.

[12] D. Mumford, J. Shah, "Optimal approximation by piecewise smooth function and associated variational problems," *Communication on Pure and Applied Mathematics*, 1989, 42, 577-685.

[13] C.M. Li, C. Kao, J. Gore, Z. Ding, "Implicit active contours driven by local binary fitting energy," in: *IEEE Conference on Computer Vision and Pattern Recognition*, 2007.

[14] Tsai, A. Yezzi, A.S. Willsky, "Curve evolution implementation of the Mumford–Shah functional for image segmentation, denoising, interpolation, and magnification," *IEEE Transaction on Image Processing*, 2001, 10, 1169-1186.

[15] L.A. Vese, T.F. Chan, "A multiphase level set framework for image segmentation using the Mumford–Shah model," *International Journal of Computer Vision*, 2002, 50, 271-293.

[16] R. Ronfard, "Region-based strategies for active contour models," *International Journal of Computer Vision*, 2002, 46, 223-247.

[17] N. Paragios, R. Deriche, "Geodesic active regions and level set methods for supervised texture segmentation," *International Journal of Computer Vision* 2002, 46, 223-247.

[18] T.T. Tran, V.T. Pham, Y.J. Chiu, K.K. Shyu, "Image Segmentation based on Geodesicaided Chan-Vese Model," in: *Proc. of the 3rd IEEE International Conference on Computer Science and Information Technology*, Chengdu, *2010, 1, 315-317.* DOI:10.1109/ICCSIT.2010.5563751.

[19] T. Liu, H. Xu, W. Jin, Z. Liu, Y. Zhao, W. Tian, "Medical Image Segmentation Based on a Hybrid Region-Based Active Contour Model," *Computational and Mathematical Methods in Medicine, 2014:10 pages*,, Article ID 890725. DOI:10.1155/2014/890725.

[20] C. Li, CY. Kao, JC. Gore, Z. Ding, "Implicit active contours driven by local binary fitting energy". In: *Proceedings of the IEEE Computer Society Conference on Computer Vision and Pattern Recognition (CVPR'07)*, 2007, p.1-7.

[21] C. Li, C. Kao, JC. Gore, Z. Ding, "Minimization of Region-Scalable Fitting Energy for Image Segmentation." *IEEE Transactions on Image Processing, 2008*; 17(10):1940±1949. https://doi.org/10.1109/TIP.2008. 2002304 PMID: 18784040.

[22] L. Wang, L. He, A. Mishra, C. Li, "Active contours driven by local Gaussian distribution fitting energy." *Signal Processing, 2009*, 89(12), 2435-2447.

[23] K. Zhang, H. Song, L. Zhang, "Active contours driven by local image fitting energy", *Pattern Recognition,2010*, 43(4), 1199-1206. https://doi.org/10.1016/j.compmedimag. 2009.04.010 PMID: 19482457.

[24] K. Zhang, L. Zhang, H. Song, W. Zhou, "Active contours with selective local or global segmentation: A new formulation and level set method." *Image and Vision Computing*, 2010, 28(4), 668±676. https://doi.org/10.1016/j.imavis.2009.10.009.

[25] F. Akram, J. Kim, HU. Lim, KN. Choi, "Segmentation of Intensity Inhomogeneous Brain MR Images Using Active Contours." *Computational and Mathematical Methods in Medicine, 2014*, 194614:1-194614:14. https://doi.org/10.1155/2014/194614 PMID: 25143780.

[26] G. Aubert, P. Kornprobst, "Mathematical Problems in Image Processing: Partial Differential Equations and the Calculus of Variations." *2nd ed. Springer Publishing Company, Incorporated.* 2010.

[27] X. Li, D. Jiang, Y. Shi, W. Li, "Segmentation of MR image using local and global region based geodesic model," *Biomedical engineering online*, 2015, 14(1), p8. DOI:10.1186/1475-925X-14-8.

[28] F. Akram, J. Kim, C. Lee, KN. Choi, "Segmentation of Regions of Interest Using Active Contours with SPF Function." *Computational and Mathematical Methods in Medicine. 2015*; :710326:1±710326:14.(2015) https://doi.org/10.1155/2015/710326 PMID: 26078780.